THE RESPONSE OF PRIMITIVE EQUATION MODELS TO THERMAL AND/OR MECHANICAL FORCING

W. Wergen

European Centre for Medium Range Weather Forecasts

Reading, U.K.

ABSTRACT

The efficiency of thermal and mechanical forcing in global, baroclinic primitive equation models is investigated. The dependence on the horizontal scale and vertical structure, as well as on the latitude and time scale of the forcing, is discussed. The impact of the static stability of the atmosphere is examined. Some of the theoretical results are verified in forecast experiments.

1. INTRODUCTION

Currently there is controversy as to the role of mechanical and thermal forcing in maintaining the quasi-stationary large scale flow. For instance, Lin (1982) concludes that topographic forcing is dominant, whereas Huang and Gambo (1982) find that the response to heat sources is larger than the response to topography. Held (1983) obtains roughly equal sensitivity to thermal and orographic forcing. In a recent paper, Jacqmin and Lindzen (1983) report experiments which 'decisively' show that orography is the major forcing mechanism; also Wallace et al. (1983) demonstrated how the use of an enhanced orography can result in a reduction of systematic forecast errors.

While the majority of results seems to support the importance of topography, it is not clear why different authors arrive at different conclusions. In this paper we shall try to shed some light onto this problem by investigating the interaction between the dynamical and the parameterised physical processes in a forecast model. In Section 2 some of the systematic forecast errors of the ECMWF model will be reviewed. The normal mode concept will be used to derive expressions for the efficiencies of thermal and mechanical forcing in Section 3. In the last section there will be a discussion about how these results can be applied in the interpretation of forecast experiments with a modified mass and/or wind field forcing.

2. REVIEW OF FORECAST ERRORS

An interesting feature of the forecast errors of the ECMWF model is their approximately linear growth rate in time during the early stages of the forecast. This was noted by Wallace et al. (1983). The relative contribution of analysis and model errors to this type of total forecast error has recently been investigated by Arpe et al. (1984). They conclude that the rms amplitudes of the model errors grow linearly in time up to day 4 to 5 of the forecast. Yet another indication of this linear error growth is given in Fig. 1, which shows the winter mean error in the zonal mean of the zonal wind component for successive forecast intervals. Already after 12 hours the typical error pattern is established. With increasing the forecast range this pattern continues to grow approximately linearly. The dominant feature is the strong negative error in the tropical upper atmosphere. In middle latitudes, the strength of the westerlies is overpredicted and furthermore there is a large barotropic component to the error. As might be expected, the error is largely in the balanced part of the flow. This is evident from Fig. 2 which shows that the zonal mean error for the geostrophic component of the zonal wind in the northern extra-tropics is very similar to the corresponding total field in Fig. 1. There are also large linearly growing tropical forecast errors in the balanced part of the flow. Wergen (1983) discussed how erroneous physical forcing prevents some large scale Rossby modes from travelling westward as predicted by linear theory.

Problems in the interaction of the physical forcing and the dynamics are not confined to the largest scales; there are also indications of problems close to the smallest resolvable scales of the model. Fig. 3 shows a vertical cross-section for wind and potential temperature in a 6 hour forecast verifying on 11.12.1980, 12GMT along the line (0°, 95°E) to (40°S, 145°E). The forecast model has generated very intense vertical velocities over

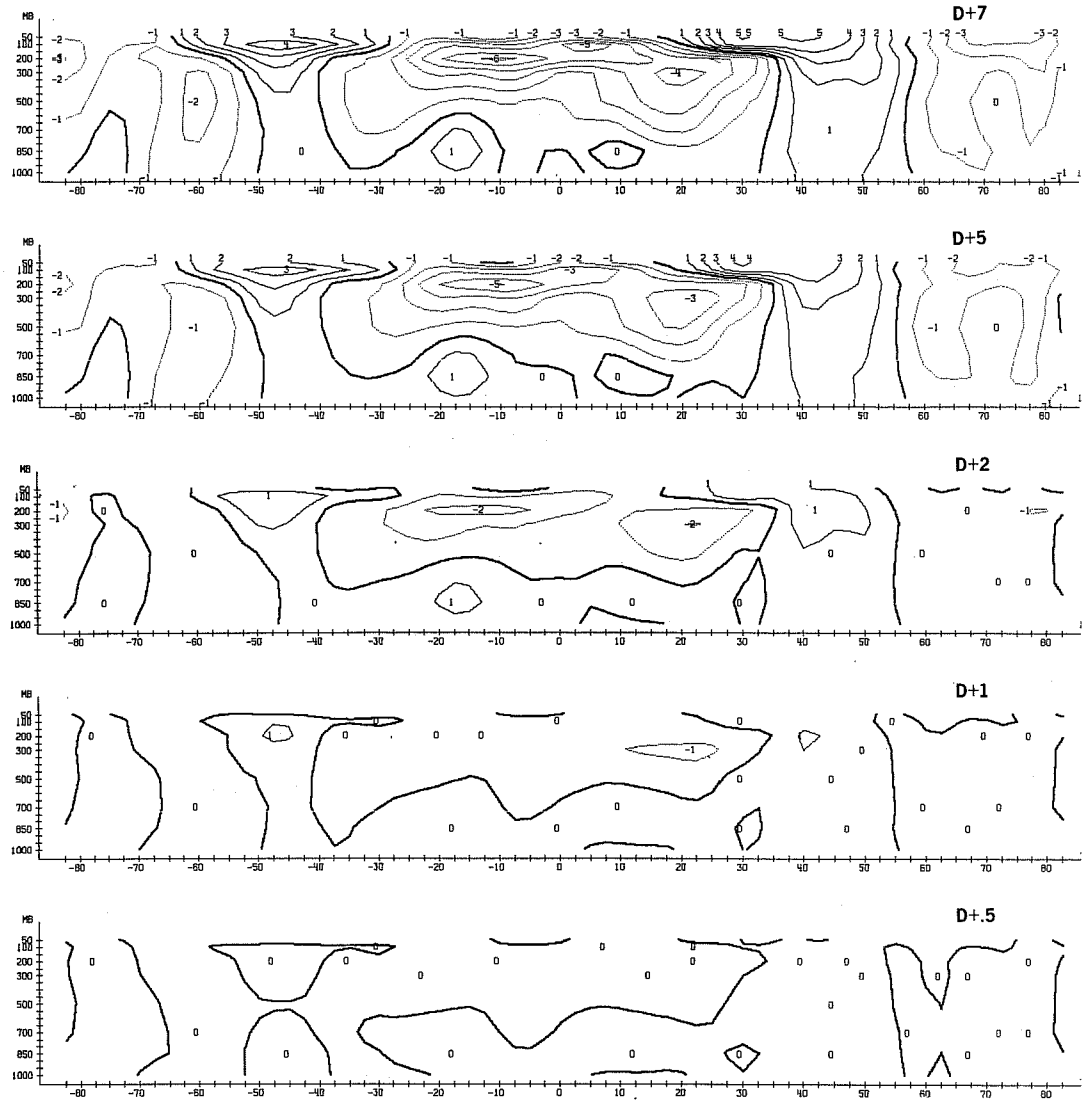

Fig. 1 Cross-section of zonal mean error in zonal wind component, averaged over all winter forecasts 81/82 and 82/83. Contour interval is 1m/sec. Panels are for 12 hour, 1 day, 2 day, 5 day, 7 day forecasts (bottom to top).

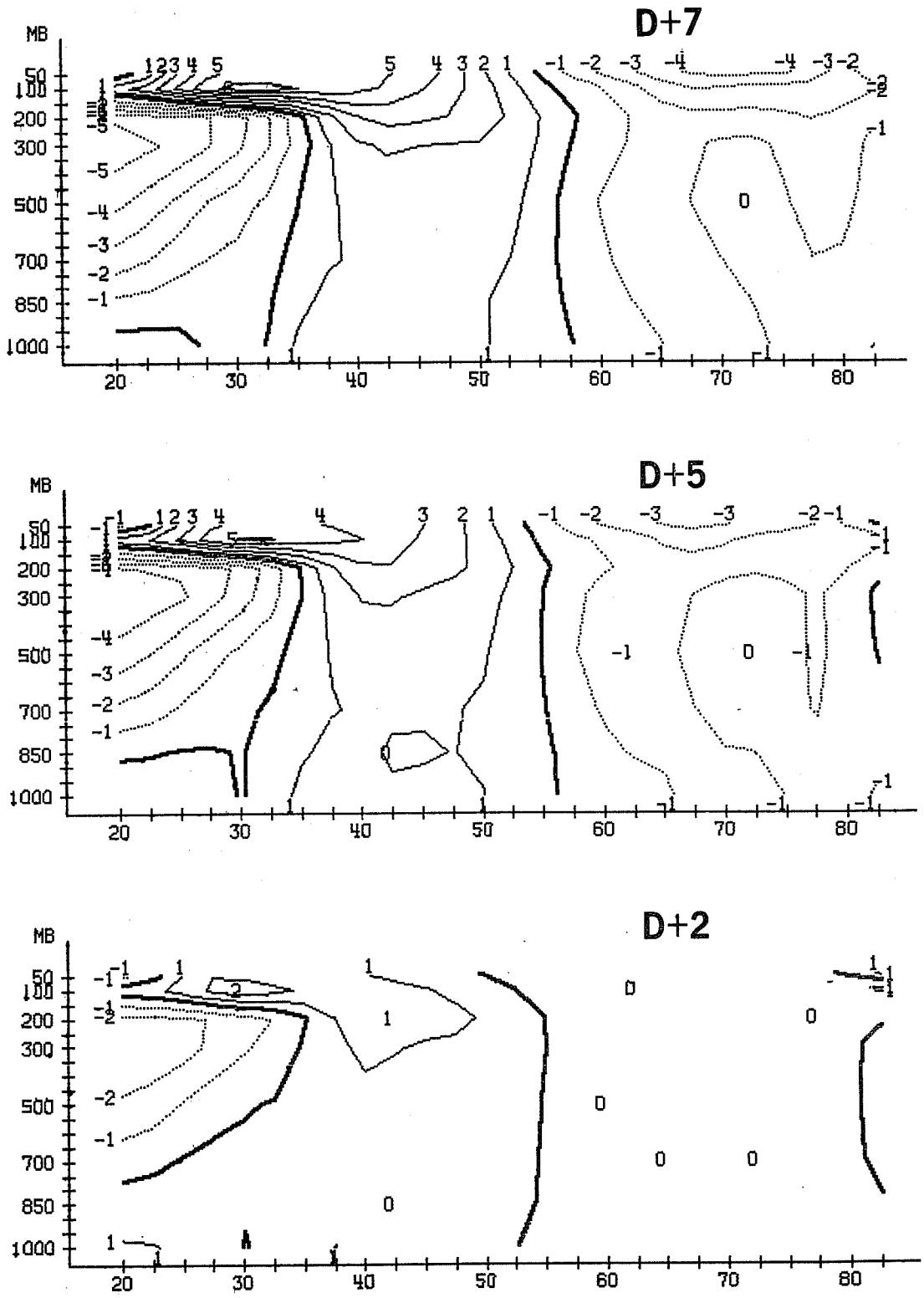

Fig. 2 Cross-section between 20°N and 90°N of zonal mean error in geostrophic zonal wind component, averaged over all winter forecasts 81/82 and 82/83. Contour interval is 1 m/sec. Panels are for 2,5 and 7 day forecasts (bottom to top).

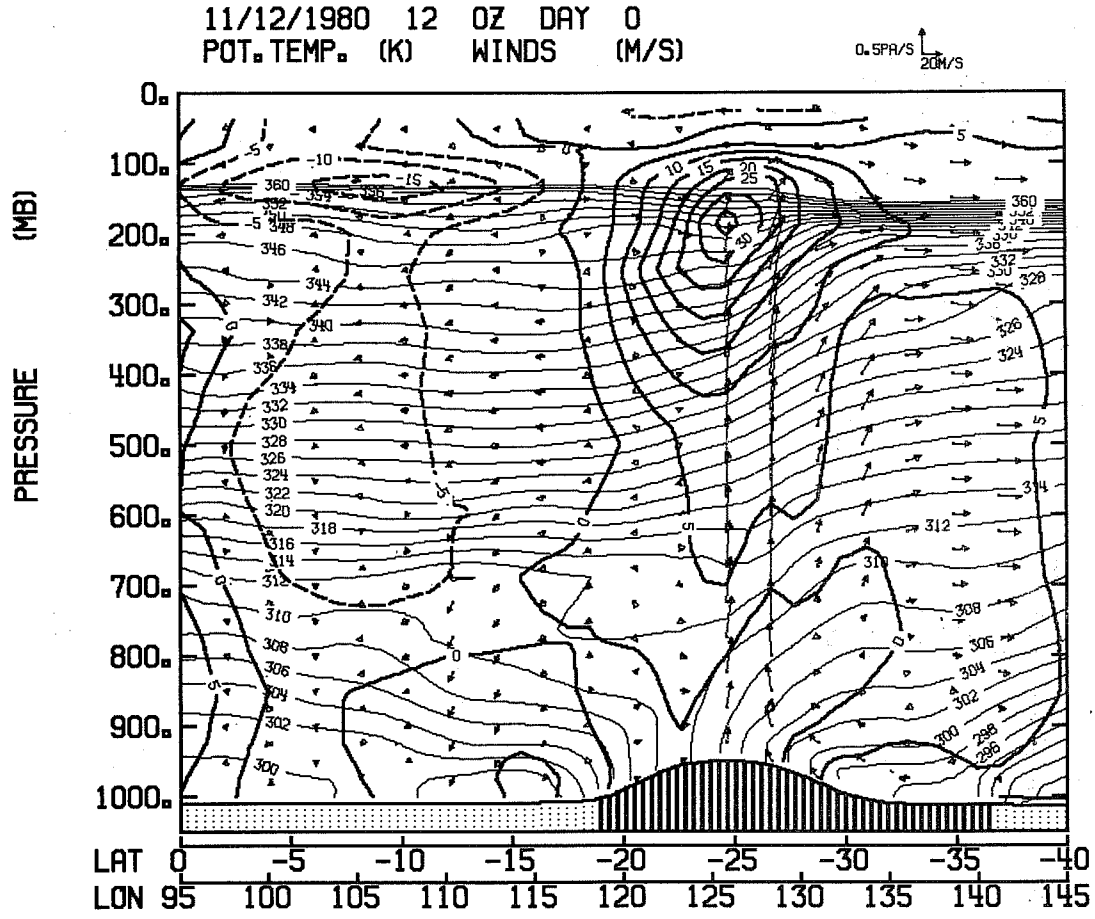

Fig. 3 Vertical cross-section of potential temperature (light) and winds from 0°, 95°W to 40°S, 145°W. Heavy lines give the wind speeds for the winds orthogonal to the intersection, positive for flow "into" the page.

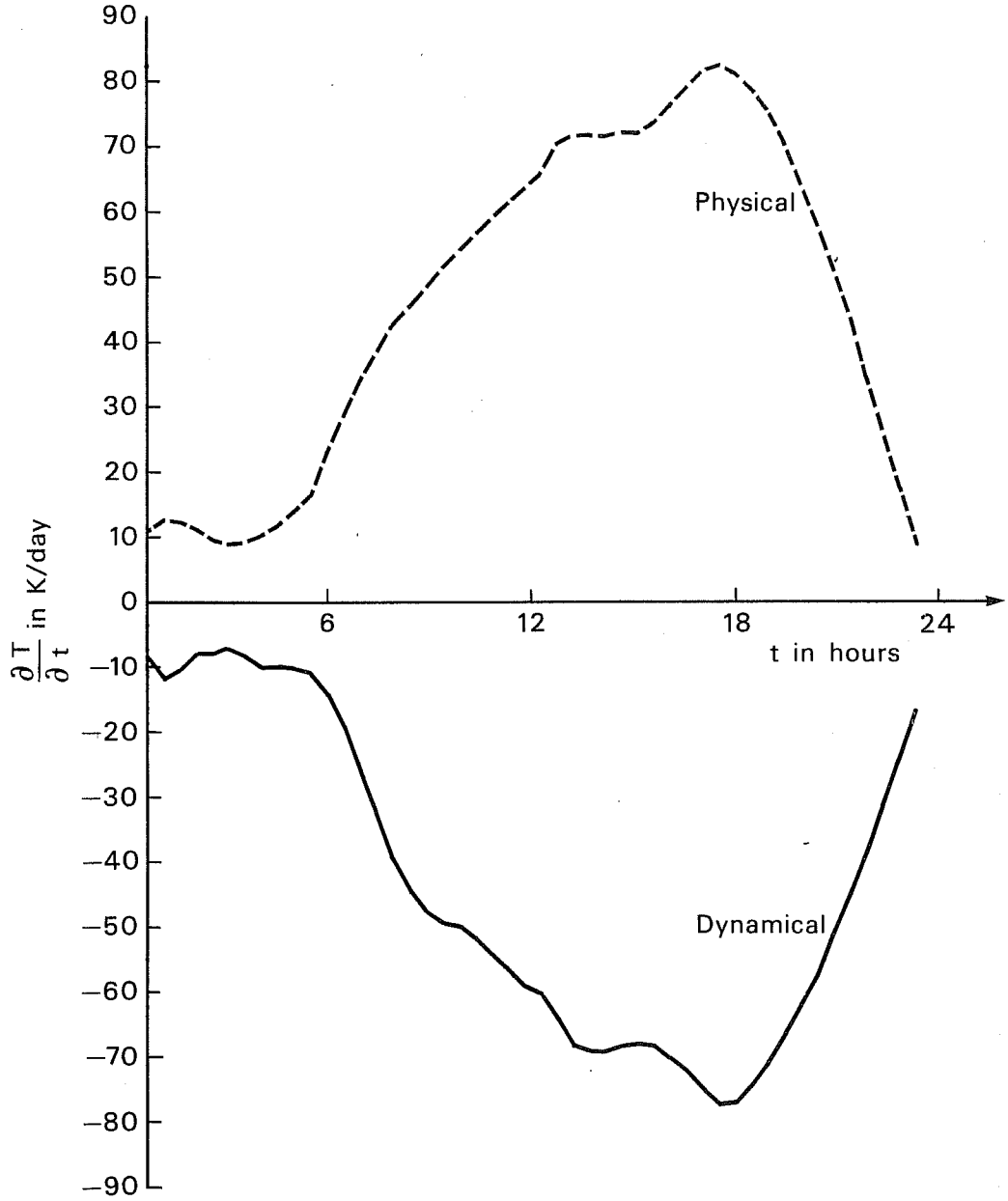

Fig. 4 Time evolution of physical and dynamical tendencies in an intense convective system at 25°S, 127°W at model level 5 (250 hpa).

Australia in a region of strong convective activity. In some cases, vertical velocities up to 2 Pa/sec can be found. These very intense systems can appear at all stages of the forecast, but they tend to die out after typically one day. They occur in both the grid-point and the spectral model. As discussed by Bengtsson et al. (1982), these systems can have a ratio of divergence to vorticity of the order of 10 in the development stage, whereas observations (Ruprecht and Gray, 1976) indicate a ratio of 0.5. A comprehensive discussion of a number of other unrealistic features of these systems is given by McBride (1984).

It is instructive to examine the interaction between dynamical and physical processes within such a system. Fig. 4 shows the time evolution of the physical (full) and dynamical (dotted) tendencies of the temperature at model level 5 (250 hpa) at a specific grid-point. The physical tendencies include the effects of radiation, turbulent fluxes and of convective heating. The first two contribute less than 1% of the total physical forcing. The dynamical tendencies are the sum of horizontal and vertical advection, and of the cooling due to adiabatic expansion; the last two terms dominate. As is apparent from Fig. 4, the physical and dynamical tendencies tend to balance each other. Rather than achieving a rapid stabilisation of the atmosphere, convection is balanced by dynamical processes due to vertical motion. Thus the model essentially "rejects" the convective signal. A possible explanation for this behaviour could be that there is an excessive excitation of the divergent circulation by convective heating in the model. If more of the convective signal went into the rotational flow, less vertical motion and therefore also less dynamical cooling would be induced, which would result in a more effective stabilisation of the atmosphere.

It is tempting to speculate that the errors described above have one common cause - namely an incorrect partitioning between the forcing of the rotational

and the divergent flow by the physical processes. Or, to put it differently, we must ask: to what extent do present parameterisation schemes influence the weather (Rossby modes) and to what extent do they simply excite noise (inertia-gravity waves)? Errors in the partitioning between the forcing of Rossby and inertia-gravity modes could not only account for the linear error growth of the balanced flow in the early part of the forecast, but also for the rejection of forcing information. In the next section, we shall investigate the relative contributions made by thermal and mechanical forcing in exciting the balanced part of the flow.

3. THE RELATIVE EFFICIENCY OF THERMAL AND MECHANICAL FORCING

In the following, we shall concentrate on the early stages of the forecast when the errors in the balanced flow still grow approximately linearly. Later in the forecast, nonlinear processes and the complicated interactions between the forcing and the flow itself result in a complex error pattern which is usually very difficult to interpret. Still later in the forecast, the models tend to reach a state which can be regarded as a model climate. The growth of the difference between this model climate and the observed one is sometimes called the "climatic drift" of the model. This drift problem will not be explicitly addressed here. At present it is not clear how the climatic drift is related to the errors occurring in the very early part of the forecast.

3.1 The model equations in Rossby mode space

In order to investigate the linear error growth in the balanced flow, it is convenient to use the normal mode concept to project the model equations into Rossby mode space. A similar procedure, except for gravity modes, is used in the nonlinear normal mode initialisation. The technical details are not of interest here - they can for instance be found in Daley (1981).

The model equations for a baroclinic, global, primitive equation model in Rossby mode space can be written as:

$$\frac{dR^k_{m,n}}{dt} = i\nu^k_{m,n} R^k_{m,n} + D^k_{m,n} \qquad (1)$$
$$+ \langle w_u{}^k_{m,n} F_u{}^k_m \rangle + \langle w_v{}^k_{m,n} F_v{}^k_m \rangle + \langle w_T{}^k_{m,n} F_T{}^k_m \rangle$$

where $R^k_{m,n}$ is the amplitude of a particular Rossby mode for zonal wavenumber m, meridional index n and vertical mode number k; $\nu^k_{m,n}$ is its free frequency. The first term on the right hand side describes the contribution of the linear tendencies to the time rate of change of $R^k_{m,n}$, while $D^k_{m,n}$ represents the projection of the sum of all nonlinear dynamical tendencies on the Rossby mode in question. The sum of the last three terms in (1) is the projection of the physical tendencies consisting of zonal and meridional momentum forcing F_u and F_v, and the diabatic forcing F_T. The inner product, indicated by $\langle\ \rangle$, describes the meridional projection of the forcing terms onto Rossby mode with meridional index n, once the zonal and meridional transforms have already been done. As can be seen from (1), a Rossby mode can be excited by both mechanical (F_u,F_v) and thermal (F_T) forcing. The relative contribution of the individual processes to the total physical forcing of the mode is determined by the weights w_u, w_v and w_T. For instance, a large diabatic forcing F_T will not necessarily be efficient in that sense, as it might be coupled with a very small weight w_T. Its effect is then to excite gravity waves which rapidly disperse the information away from the source before they are finally damped out in the model. In a linear context, the effect of the forcing is thus largely lost. It is only by nonlinear interactions between Rossby and gravity waves, and between gravity waves and the parameterisation schemes, that some of the information can be kept in the Rossby regime.

The weights w_u, w_v, and w_T are just the wind and mass field configurations of

the Rossby mode in question. The mere fact that the model equations can be written as in (1) means that the concepts used in data assimilation theory (Daley, 1980) or in geostrophic adjustment theory (Blumen, 1972) can also be used in this context. Therefore the Rossby mode projection of a forcing from a particular parameterisation scheme can be computed in the same way as the Rossby mode projection of an atmospheric state. Similar to an observation not being accepted by a model, forcing information can also be rejected if the signal goes mainly into the gravity mode regime. In the tropics, the correct specification of the initial wind field is important for deterministic forecasting (Daley, 1980). Tropical mass field information will largely be ignored. In the following we shall investigate the conditions under which forcing information is accepted or rejected by a primitive equation model.

We shall call a forcing "efficient" if it gets a large weight w in forcing Rossby modes, and consequently a small weight in forcing inertia-gravity modes. An efficiency parameter η_M of mechanical forcing can thus readily be defined:

$$\eta_M = \frac{(w_u{}^k_{m,n})^2 + (w_v{}^k_{m,n})^2}{(w_u{}^k_{m,n})^2 + (w_v{}^k_{m,n})^2 + (w_T{}^k_{m,n})^2} \qquad (2)$$

The efficiency of thermal forcing then becomes:

$$\eta_T = 1 - \eta_M \qquad (3)$$

Both η_M and η_T vary between 0 and 1. A large value of η means that this particular forcing is efficient in exciting Rossby modes, and consequently does not force gravity waves; a value close to 0 indicates an inefficient forcing in this sense, because it mainly excited gravity waves. Note from (3) that if mechanical forcing is efficient, thermal forcing is inefficient and vice versa. The definition (2) is equivalent to the ratio of kinetic to total (kinetic + available potential) energy for a normal mode. This quantity,

albeit globally integrated, was first discussed by Longuet-Higgins (1968). In order to determine the weights w, we have to find the normal modes of a forecast model, i.e. we have to find the eigensolution of the linearised model equations. This task can easily lead to very large matrix problems. In order to end up with sizeable matrices, it is necessary to assume rather simple basic states in the linearisation process. In the following we shall use two models in which the basic state has been assumed to be at rest and the temperature distribution depends only on the vertical coordinate.

3.2 Vertical projection

When dealing with multi-level models, one has to consider the vertical as well as the horizontal structure of the forcing. For a simple basic state at rest, the linearised model equations can be separated into a vertical and a horizontal part (Daley 1981). The vertical analysis yields a complete set of eigenvalues (equivalent depths) and eigenvectors (vertical modes). Every equivalent depth is related to a specific vertical mode describing the vertical structure of mechanical and thermal forcing. Fig. 5 shows the first 5 vertical modes for the ECMWF model, computed for an isothermal basic state. (The equivalent depths for these modes may be found in Table 2 in Sect.3.5). The first vertical mode describes the barotropic part of the flow; its equivalent depth is 11.89 km. The second vertical mode changes sign near the tropopause, whilst the third and fourth vertical modes account for structures which change sign in the troposphere. In general, vertical mode k has k-1 sign changes. With increasing order k the region of maximum amplitudes moves towards lower levels. Therefore the higher vertical modes represent only shallow structures close to the lower boundary.

It is instructive to examine how the observed diabatic heating rates for composite tropical disturbances (Thompson et al., 1979) project on these vertical modes. Table 1 gives the amplitudes of the first five vertical modes

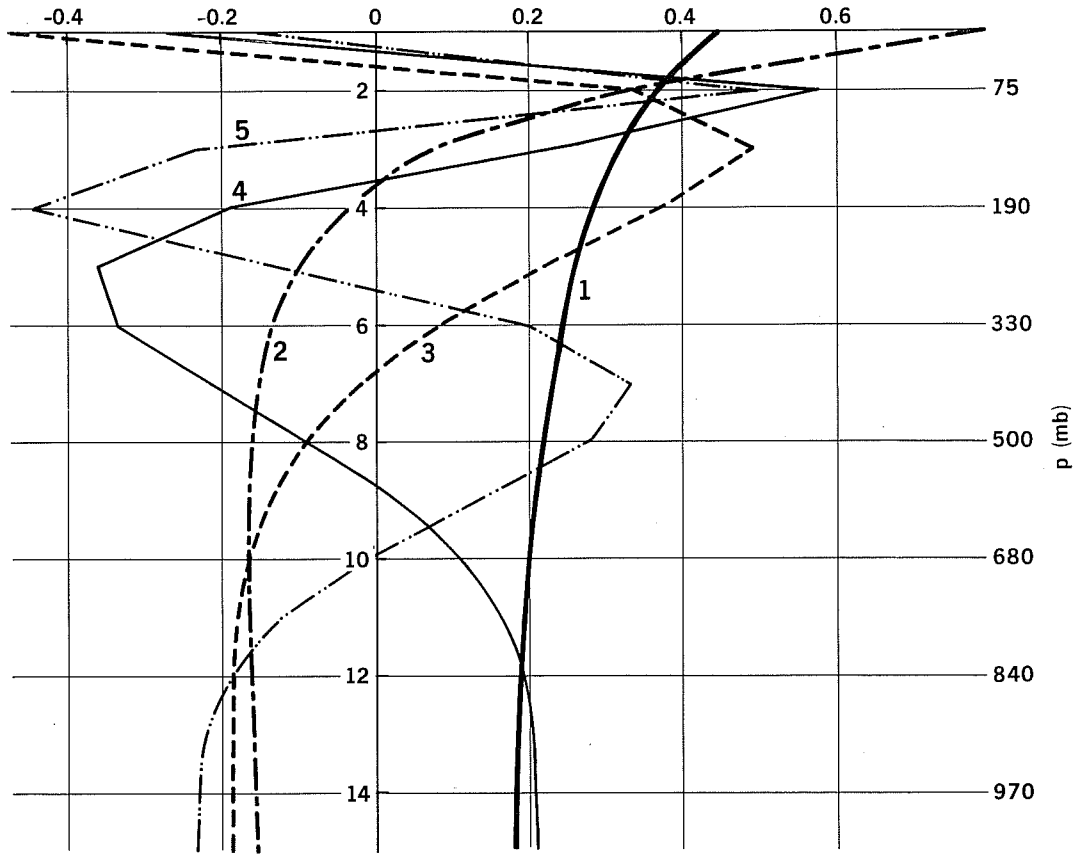

Fig. 5 Vertical structure of first 5 vertical modes for the 15 level ECMWF model with an isothermal (300K) basic state.

for the Marshall Island (West Pacific) and GATE (East Atlantic) data sets. All values have been normalised by the amplitude of the external mode.

Vertical mode	Marshall Island	GATE
1	1.00	1.00
2	- .64	-.95
3	.19	-.71
4	.63	.08
5	.50	.37

Table 1. Amplitudes of a projection of observed (Thompson, 1979) diabatic heating for the Marshall Island (left) and GATE (right) datasets on the first 5 vertical modes of the ECMWF model.

For both datasets, the barotropic contribution dominates. The combination of the first two modes accounts for the constant tropospheric but very small stratospheric part. Large amplitudes can further be found for the third (East Atlantic) and fourth (West Pacific) vertical modes. As we shall see later, the relative projection of the vertical profile of diabatic heating onto the vertical modes has consequences for the efficiency of the heating in a forecast model.

3.3 Mid-latitude f-plane model

After the forcing has been projected onto the vertical modes, the vertical and horizontal problems can be treated separately. For each vertical mode we have to consider a shallow water type model in the horizontal with the equivalent depth of the vertical problem as mean depth of the fluid. Particularly simple expressions for η_M can be obtained for a f-plane model. Assuming bi-periodic boundary conditions, the model variables can be expanded in double Fourier series.

$$\begin{bmatrix} u \\ v \\ \phi \end{bmatrix} = \sum_{m,\ell} \begin{bmatrix} u_m^{\ell} \\ iv_{m_{\ell}}^{\ell} \\ \sqrt{\bar{\phi}_k}\phi_m^{\ell} \end{bmatrix} e^{i(mx+\ell y)} \qquad (4)$$

Here m and ℓ are zonal and meridional wavenumbers, and $\bar{\phi}_k$ is the equivalent depth of the vertical mode k under consideration. Using (4), the weights w can be computed analytically for a model linearised around a basic state at rest. They are given by (Wergen, 1981).

$$\begin{bmatrix} w_u \\ w_v \\ w_T \end{bmatrix} = \begin{bmatrix} -i\ell\sqrt{\bar{\phi}_k} \\ m\sqrt{\bar{\phi}_k} \\ f_o \end{bmatrix} \qquad (5)$$

Here f_o is the constant Coriolis parameter. The weights for mechanical forcing w_u and w_v increase with decreasing horizontal scale and increasing equivalent depth $\bar{\phi}_k$. The weight for thermal forcing w_T increases with latitude.

An efficiency of mechanical forcing η_M^* can easily be computed.

$$\eta_M^* = \frac{(\ell^2 + m^2)\,\bar{\phi}_k}{(\ell^2 + m^2)\,\bar{\phi}_k + f_o^2} \qquad (6)$$

The definition (6) differs from (2) in that η_M is an explicit function of latitude, whereas in η_M^* the assumption of a constant f_o allowed the elimination of the meridional dependence by a Fourier transform. Thus, η_M^* is a function of the horizontal wavenumbers ℓ and m and of the vertical mode number k. Fig. 6 shows η_M^* as a function of (two-dimensional) horizontal wavelength and equivalent depth for 60° (left) and 30° (right) latitude. The most striking feature in both graphs is the large area of pre-dominance of mechanical forcing. For barotropic structures mechanical forcing is the more efficient process, irrespective of horizontal scale. The same conclusion

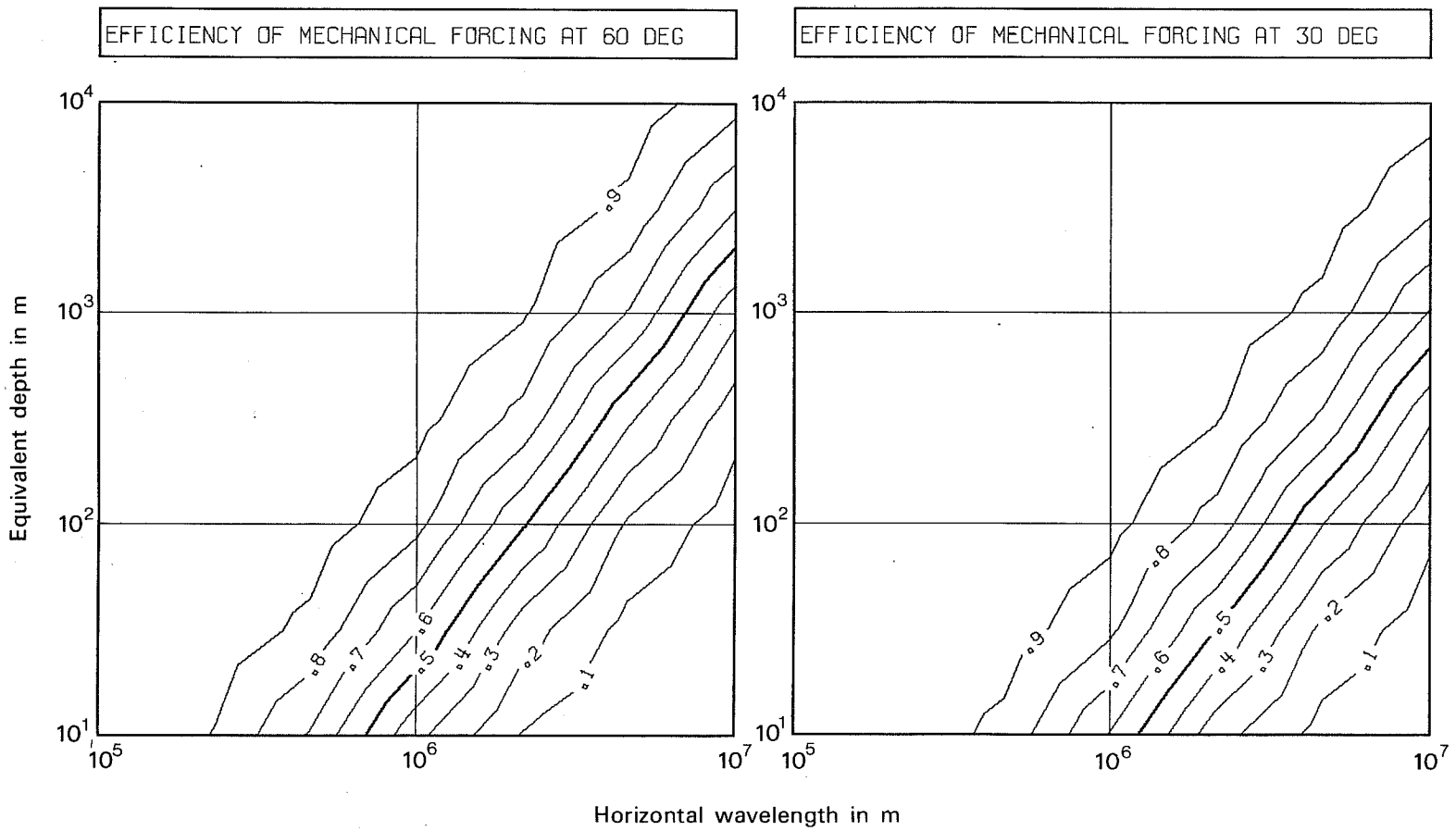

Fig. 6 The efficiency of mechanical forcing η_M^* for a f-plane model at 60° (left) and 30° (right) latitude as a function of twodimensional horizontal wavelength (abscissa) and equivalent depth (ordinate).

holds - independent of the vertical structure - for all horizontal scales smaller than 10^3 km. Only for shallow vertical, but large horizontal scales is thermal forcing the more efficient mechanism. The pre-dominance of mechanical forcing becomes even more pronounced in lower latitudes. These results agree with a study by Schubert et al. (1980) who showed that for an axisymmetric vortex with a radius of 300 km on a f-plane heating contributes very little in producing balanced flow.

When interpreting the numbers in Fig. 6 quantitatively, the simplifications in the underlying model (basic state at rest, f-plane, bi-periodic boundary conditions) should be kept in mind. However, the graphs show qualitatively how η_M^* depends on horizontal scale, vertical structure and latitude.

This simple calculation of the efficiency of mechanical forcing ignores one important aspect of the problem. From (5) it is evident that the weights w_u and w_v are the spectral equivalent to meridional and zonal partial derivatives - apart from scaling factors. Therefore, the Rossby mode component of the mechanical forcing can be expressed as:

$$w_u F_u + w_v F_v = \sqrt{\bar{\phi}_k}\ \left(-\frac{\partial}{\partial y} F_u + \frac{\partial}{\partial x} F_v\right) \qquad (7)$$

This means that the mechanical forcing has to have a rotational component in order to force Rossby waves. A purely divergent forcing would not impact on the balanced flow. This is equivalent to saying that the mechanical forcing has to act on the vorticity field in order to be efficient. For scales where η_M^* is large, this is an important additional necessary condition for the efficency of mechanical forcing.

3.4 Global model

In order to apply the concepts outlined in the previous sections to a global model, one needs to compute the normal modes for such a model. This can be

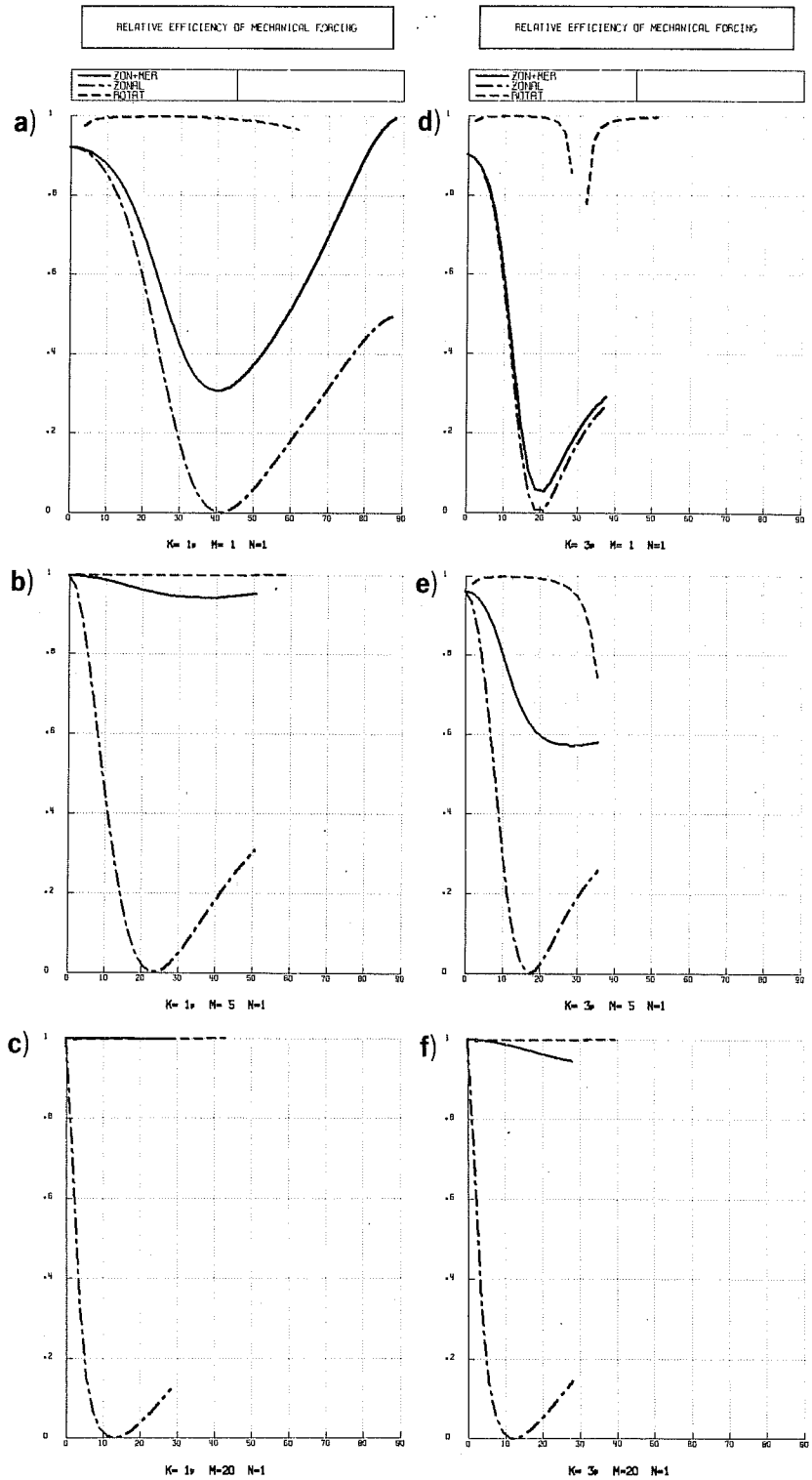

Fig. 7 Efficiency η_M of mechanical forcing (full), of zonal mechanical forcing η_{MZ} (dashed-dotted) and rotational parameter r (dashed) as function of latitude for gravest symmetric (n=1) Rossby modes. a) external, zonal wavenumber 1 ; b) external, zonal wavenumber 5, c) external, zonal wavenumber 20, d) second internal, zonal wavenumber 1, e) second internal, zonal wavenumber 5, f) second internal, zonal wavenumber 20.

done in the same way as in the normal mode initialisation process (Temperton and Williamson, 1981). In the following, we shall use the normal modes of the ECMWF multi-level, global grid-point model, derived for an isothermal (300K) basic state at rest.

Many properties of these modes have been discussed by Kasahara (1976). There are different weight vectors w_u, w_v, w_T for each zonal wavenumber m, meridional index n and vertical mode k. Each vector describes the latitudinal dependence of the wind or mass field of the mode. The efficiency parameter η_M can easily be computed and Fig.7 gives some results for various Rossby modes.

a) External Rossby modes

The full line in Fig. 7a shows η_M as a function of latitude for a zonal wavenumber 1, gravest symmetric (n=1), external (k=1) Rossby mode. As the free period of this mode is 5 days, this mode is sometimes called the "5-day wave". As can be seen, in the tropics this planetary scale mode is mostly influenced by mechanical forcing; in mid-latitudes, mechanical and thermal forcing are roughly equally important. The renewed increase in η_M towards the pole is somewhat misleading in this diagram, as all weights become small at higher latitudes for this mode. The dashed-dotted curve in Fig. 7a shows the efficiency of zonal mechanical forcing η_{MZ}, defined by:

$$\eta_{MZ} = \frac{(w_{u\ m,n}^{k})^2}{(w_{u\ m,n}^{k})^2 + (w_{v\ m,n}^{k})^2 + (w_{T\ m,n}^{k})^2} \qquad (8)$$

In the tropics the mechanical forcing is only required in the zonal wind in order to be efficient for this barotropic mode. At higher latitudes, the predominance of zonal mechanical forcing diminishes. The dashed curve in Fig. 7a shows the parameter r, defined by

$$r = \frac{\left(-\frac{\partial w_u}{\partial y} + \frac{\partial w_v}{\partial x}\right)^2}{\left(-\frac{\partial w_u}{\partial y} + \frac{\partial w_v}{\partial x}\right)^2 + \left(\frac{\partial w_u}{\partial x} + \frac{\partial w_v}{\partial u}\right)^2} \qquad (9)$$

(Values with a denominator smaller than 10^{-2} in the definitions of η_M, η_{MZ}, and r are not plotted). The variable r is the ratio of squared vorticity over the sum of squared vorticity and divergence of the weights. A value of r close to 1 indicates that the mode is largely rotational, which means that the mechanical forcing terms have to have a rotational component in order to project on that mode. As we found already for the f-plane model, the need for a rotational component is an important extra condition when discussing the efficiency of mechanical forcing in exciting Rossby modes. Fig. 7b gives the same curves, but for the gravest symmetric (n=1), external (k=1), zonal wavenumber m=5 Rossby mode. For this medium scale, barotropic mode, mechanical forcing is the dominant process at all latitudes. In the extra-tropics, forcing of the meridional wind component becomes more efficient. Again, the mechanical forcing has to have a rotational component in order to be effective. For a small scale (m=20), external Rossby mode we find $\eta_M \approx 1$ for all latitudes (Fig. 7c). For external modes with still smaller scales η_M and r are practically identical to unity, which means that these modes can only be excited by rotational mechanical forcing. Thermal forcing on these scales would only generate gravity waves.

b) Internal Rossby modes

The corresponding set of curves for the second internal (k=3), gravest symmetric (n=1), zonal wavenumber m=1 Rossby mode are given in Fig. 7d. The equivalent depth of this mode is 947m. This large scale, internal mode is equatorally trapped. The relative efficiency of mechanical forcing η_m decreases rapidly with increasing latitude, which means that diabatic forcing

away from the equator is generally more efficient for this large scale, baroclinic mode. For a smaller scale, baroclinic mode (k=3,n=1,m=5) in Fig. 7e, mechanical forcing is roughly equally important as diabatic forcing. As for the external mode, we have a tendency of increased efficiency of mechanical forcing with decreasing horizontal scale. Fig. 7f shows that for a small scale (m=20) baroclinic (k=3) mode, rotational mechanical forcing is the dominating process. Still smaller internal Rossby waves are exclusively influenced by mechanical forcing. With decreasing equivalent depth, more modes become thermally influenced at the long wave end of the spectrum. For the small scales, there remains always the dominance of mechanical forcing. As we saw in section 3.2 the observed diabatic heating profile has a large projection on internal modes. From Fig. 7d-f one would conclude that the large scale organisation of this heating is more important than its small scale structure. On smaller horizontal scales, the correct modelling of momentum transport is important, be it by convection or by breaking gravity waves. Only for the high vertical modes describing shallow structures, can the thermal forcing be expected to be dominant also on smaller horizontal scales; this has also been reported by Tiedtke (1983).

c) Mixed Rossby-gravity and Kelvin modes

So far, the results obtained from a global model agree by and large with the findings for a simple f-plane model. For a global model there are, however, additional modes not present in a simple f-plane theory, namely the mixed Rossby-gravity mode and the Kelvin mode. These modes are unique as neither from their relation between mass and wind field, nor from their frequency characteristics, can they be classified as Rossby or as inertia-gravity modes. A detailed discussion of these modes can be found in Matsuno (1966). The efficiency curves for an external (k=1), zonal wavenumber m=1, mixed Rossby-gravity mode are shown in Fig. 8a. This mode is anti-symmetric around

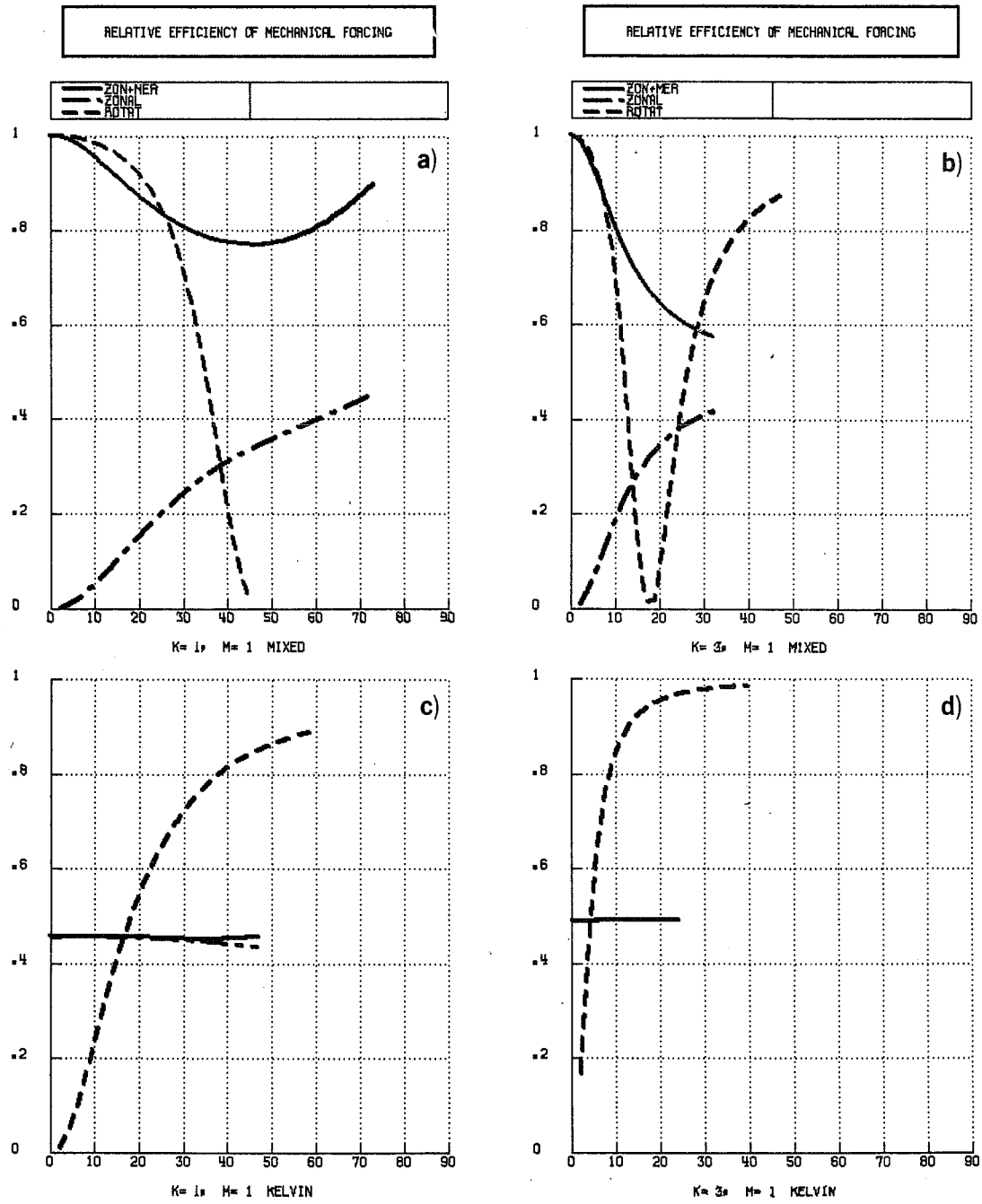

Fig. 8 Similar to Fig. 7, but for external (a) and second internal (b) mixed Rossby-gravity mode and for external (c) and second internal (d) Kelvin mode. Zonal wavenumber is always one.

the equator with respect to mass and zonal wind field. Mechanical forcing is clearly the most important process for this mode. As it describes cross-equatorial flow, meridional momentum forcing in the tropics is essential. The importance of a rotational component in the forcing decreases with higher latitudes. Roughly the same conclusions apply for an internal (k=3) zonal wavenumber m=1 mixed mode (Fig. 8b).

The prominent feature of Kelvin modes (Fig. 8c, 8d) is their equal sensitivity to mechanical and diabatic forcing. η_M is nearly independent of latitude, vertical structure and horizontal scale. In the tropics the rotational contribution is negligible. Mechanical forcing is confined to the zonal wind component. As Kelvin waves respond to thermal forcing irrespective of scale, they can be expected to be sensitive to convection. This has indeed been shown by Hayashi and Goulder (1978). All in all, the presence of Kelvin and mixed Rossby gravity waves adds some complications to an otherwise simple picture.

3.5 The influence of the thermal stratification

In the derivation of the normal modes for a baroclinic model, the stability of the basic state atmosphere enters only the vertical structure equation. In order to evaluate the impact of different stratifications on the results in the previous sections, it is therefore sufficient to compute the equivalent depth $\bar{\phi}$ for various static stabilities of the basic state. In Table 2 the first five equivalent depths for the 15 level ECMWF model are given for three different temperature distributions.

Vertical mode	3000K	ICAO	Near neutral
1	11,886	9,558	8,870
2	3,369	2,370	1,614
3	947	474	190
4	365	166	77
5	171	75	24

Table 2: Equivalent depths in metres for isothermal (left), ICAO (middle) and near neutral (right) basic state temperatures.

The first row shows the values for an isothermal (300K) basic state. The second row is for an ICAO atmosphere with a ground temperature of 288K and a lapse rate of -6.5 °C/km. The last row is for a near neutral lapse rate of -8.5 °C/km. For the last two cases the temperature in the three uppermost model levels has been kept constant. The results in Table 3 can be summarised by one statement: with decreasing static stability the equivalent depths decrease. As discussed in the previous section, a decreasing equivalent depth favours diabatic forcing. Thus, for the same horizontal scale and latitude, a decrease in static stability leads to an increase of the efficiency of thermal forcing.

3.6 The influence of the time scale of the forcing

So far, we have made no assumptions about the time scale of the forcing. A number of papers have dealt with the tropical response to a prescribed, specific functional form of transient diabatic heating. Silva Dias et al (1983) used a tropical β-plane model to investigate the tropical response to transient convection placed at various latitudes. Kasahara (1983) used a global model for a similar investigation. Their results can qualitatively be understood in terms of the waves excited by the diabatic forcing and their

dispersive properties. The present study is not concerned with the exact computation of the response to a particular form of diabatic forcing but rather tries to identify the conditions under which physical processes, thermal and/or mechanical, most efficiently excite Rossby, Kelvin and mixed Rossby-gravity waves.

In order to discuss the impact of the time scale of the forcing on the results obtained so far, we have to solve the model equations in normal mode space for time dependent forcing terms. Assuming periodic forcing, (1) can be re-written (dropping indices) as

$$\frac{dY}{dt} = i\nu Y + D + \langle w_u F_u \rangle e^{i\omega_u t} + \langle w_v F_v \rangle e^{i\omega_v t} + \langle w_T F_T \rangle e^{i\omega_T t} \qquad (10)$$

where $\omega_u, \omega_v, \omega_T$ are the frequencies of the zonal and meridional momentum and of the thermal forcing respectively. Y is the amplitude of an arbitrary normal mode. Excluding resonance, the solution can be expressed as:

$$Y = ce^{i\nu t} + e^{i\nu t} \int De^{-i\nu t}\, dt + \frac{\langle w_u F_u \rangle e^{i\omega_u t}}{i(\omega_u - \nu)} + \frac{\langle w_v F_v \rangle e^{i\omega_v t}}{i(\omega_v - \nu)} + \frac{\langle w_T F_T \rangle e^{i\omega_T t}}{i(\omega_T - \nu)} \qquad (11)$$

where c is an integration constant to be determined from the initial conditions. Clearly the response to the forcing, given by the last three terms in (11), is determined by two factors: the projection of the forcing on the mode in question and by the difference between the frequency of the forcing and the free frequency of the mode. The requirements for the forcing to project on Rossby, Kelvin and mixed modes have already been discussed. With regard to the frequencies, the following qualitative distinctions can be made:

a) Forcing frequency $|\omega|$ much lower than frequency $|\nu|$ of the mode

In this case, which includes stationary forcing, the response is inversely proportional to the free frequency of the mode. The lower the frequency ν, the larger the response. This favours the response of slow modes (Rossby, large scale internal Kelvin) in the case of quasi-stationary forcing.

b) Forcing frequency $|\omega|$ much larger than frequency $|\nu|$ of the mode

Here the response is inversely proportional to the frequency ν. Thus, high frequency forcing will generally have a smaller effect on slow modes than forcing which varies very slowly

c) Forcing frequency $|\omega|$ comparable to frequency $|\nu|$ of the mode

In this case the response depends critically upon the sign of ω and ν For cases close to resonance, a large response can be expected. This might be relevant for modes such as the external, smaller scale Kelvin waves and the mixed Rossby gravity waves, which have periods similar to the time scale of convective heating. For the resonant case it is easy to show that the solution grows linearly in time. This linear growth only depends on the projection of the forcing on the mode in question and not on the resonance frequency.

In conclusion it should be noted that the response of the Rossby regime depends upon the projection of the forcing and on its time scale. The response to both mechanical and thermal forcing is largest for quasi-stationary forcing of the balanced flow. Large responses can also be expected for cases close to resonance. High frequency forcing will generally result in a small response of the Rossby regime.

3.7 Discussion

It was shown how data assimilation theory can be applied in the derivation of efficiency parameters for mechanical and thermal forcing in baroclinic primitive equation models. These parameters depend on the horizontal and vertical scale of the forcing as well as on the latitude and the time scale of the forcing. They are also a function of the static stability of the atmosphere. The efficiency of mechanical forcing increases with decreasing horizontal but increasing vertical scale, whilst the efficiency of thermal forcing increases with increasing latitude.

a) Mechanical forcing

An important result of the present study is the dominance of quasi-stationary, rotational, mechanical forcing for almost all barotropic structures and on all small horizontal scales, especially in the tropics. This finding suggests that in order to improve the forecasts for these scales, a careful modelling of the mechanical forcing is more important that the parameterisation of diabatic effects. A prime factor in mechanical forcing is the role played by orography. However, it is not really clear how to adequately parameterise the orographic forcing in numerical prediction models. The concept of "parameterisation by height", as discussed by Wallace et al. (1983), results in a slowing down of the systematic error growth in the early part of the forecast. From the present study it would seem that the parameterisation of the rotational component of the vertically integrated turbulent momentum transports, i.e. the curl of the stresses at the top of the atmosphere minus the curl of the surface stresses, is important. In general, all possible smaller scale vorticity sources and sinks are worth considering. These might be related to breaking internal gravity waves or to processes responsible for clear air turbulence. There is also an implication for high resolution

modelling. The finer the resolution, the more important the exact parameterisation of the mechanical forcing in the newly resolved small scales becomes.

b) Thermal forcing

Compared to mechanical forcing, thermal forcing dominates a smaller area of the spectrum. Only for horizontally large scale, but vertically shallow structures is thermal forcing the more efficient process. Therefore, the large scale organisation of the turbulent fluxes of latent and sensible heat in the boundary layer would seem to be a critical component.

c) Thermal and mechanical forcing

Between these two extremes there is, however, a range of scales where both forcing mechanisms are equally important. This has two significant implications. Firstly, within the same physical process the impact on the mass field needs to be considered as well as the impact on the wind field. For instance, from observations (Ruprecht and Gray,1976) we know that cloud clusters are a heat- as well as a vorticity source. Yet, deep cumulus convection is often parameterised to affect the temperature field only. As we saw in section 3.2, the observed diabatic heating projects onto vertical modes for which the momentum forcing is at least as important as the thermal forcing. This suggests that a large sensitivity to vorticity transports by cloud clusters can be expected. On small horizontal scales, thermal convective forcing will only excite gravity waves (section 3.4). As discussed in section 2, the resulting divergent circulation can lead to very large vertical velocities, which in turn compensate for the convective heating by adiabatic expansion and vertical advection of temperature. Including vorticity transports in the parameterisation schemes will result in less

excitation of the divergent flow, thus leading to a better acceptance of the convective signal by primitive equation models. Another example of a process affecting both mass- and windfield is orography, which is not only an obstacle to the flow but also acts as an elevated heat source (Flohn, 1953). The ratio between the vertical diffusion coefficients for heat and momentum can also be regarded as a critical parameter as it influences the projection of the turbulent transports on fast and slow modes. The second implication of the importance of both thermal and mechanical forcing on the intermediate scales is that processes affecting the momentum should be considered in conjunction with those affecting the mass field. Although the sources might be due to entirely different mechanisms, their combined effect will be larger than that of an individual component in isolation.

d) Conflicting results from earlier studies

From the present study it would seem that the results derived from filtered models are not necessarily applicable to primitive equation models. For instance, in quasi-geostrophic models the forcing can by definition excite Rossby modes only, as gravity modes are filtered out in this type of model. This might partly explain why Huang and Gambo (1982), who used a quasi-geostrophic model, get results somewhat at variance with other investigations. Similar arguments apply to Gill (1980) and to Heckley and Gill (1984), whose "long wave" approximation restricts the response to Rossby and Kelvin modes and, moreover, renders the Rossby waves non-dispersive (as pointed out by Lim and Chang, 1983). However, where these filtered models succeed in realistically simulating observed flow patterns, they may point to the way in which to re-formulate the forcing in primitive equation models in order to get a similar excitation of Rossby modes. Apart from the differences in the models used, another reason for the conflicting results discussed in

the introduction might come from the different horizontal and vertical structures of the forcing fields used. As we saw, the response of a primitive equation model critically depends on these parameters.

e) Limitations of the present study

While the general concept of deriving efficiency parameters using a normal mode expansion of the model equations is universally applicable, the actual modes used to determine the weights w_u, w_v, and w_T suffer from several approximations. In order to end up with manageable eigenvalue problems, a simple basic state at rest with a specified stratification had to be assumed. These assumptions certainly impose limitations on a quantitative interpretation of the results. However, as shown by Kasahara (1980), the inclusion of a mean zonal flow has only a modest effect on the structures of the planetary scale modes, such as the 5-day wave. Therefore, the quantitative conclusions for these modes are probably not significantly changed by a more realistic basic state. For modes with smaller horizontal and vertical scales, however, the results presented should only be taken as qualitative indications of the dependence on scales and latitude. Schubert et al. (1980) showed that for an axisymmetric vortex on an f-plane with a radius of 300 km, the geostrophic energy generation by thermal forcing increased from 1% to 13% when including a non-resting basic state. Thus, the main conclusions concerning the inefficiency of thermal relative to mechanical forcing on small scales are not changed significantly when using a more realistic basic state. For more quantitative statements the free oscillations of a global model in spherical geometry for a non-resting basic state with vertical wind shear and a more realistic temperature distribution need to be computed. Frederiksen (1982) performed such a calculation for a two level quasi-geostrophic model in order to find the unstable modes implied by an

observed wintertime circulation. In the present context, a similar approach, albeit for the full set of modes for an unfiltered model, would allow more quantitative statements on the role of mechanical and thermal forcing on smaller scales.

4. FORECAST EXPERIMENTS

In order to determine if the findings presented so far are relevant in the context of a complex operational weather prediction model, some forecast experiments with the ECMWF grid-point model were performed. The following set-up was used: an operational 10 day forecast was chosen at random. Its 10-day zonal mean forecast error in the zonal wind and the height field was used as an additional, corrective forcing of the zonal momentum and/or height field during re-runs of the forecast. This means that at every timestep the computed tendencies of u, T, and p_s were corrected by an amount corresponding to the negative day 10 zonal mean forecast error divided by the number of timesteps. If the 10 day forecast errors are entirely caused by a linear error growth, such an approach should completely remove it. Furthermore, these experiments should show whether the statements concerning the efficiency of thermal and/or mechanical forcing are applicable in a complex forecast model. As a by-product, they should also allow some insight into the question as to what extent an improved zonal mean state leads to an improved forecast of some non-zonal waves.

Before discussing the results of these experiments, it is instructive to look at the efficiency parameter η_M for the zonal mean flow. As no Rossby modes exist for the zonal mean, a somewhat different approach for describing the zonal mean balanced flow has to be used. From the eigenvalue analysis we get multiple eigenvalues $\lambda_i = 0$ for this case. As the number of multiple eigenvalues corresponds exactly to the rank decay of the eigenvector problem,

it is always possible to construct a complete set of modes. The actual computations follow Kasahara (1977). Essentially, the eigenmodes are the solutions of the linearised, zonal mean balance equation. The zonal mean height and wind field are in geostrophic balance; the meridional wind component vanishes. These modes are sometimes referred to as "geostrophic modes".

Fig. 9 shows the curves of η_M as a function of latitude for the external, gravest symmetric (full) and antisymmetric (dashed-dotted) geostrophic modes. In the tropics, mechanical forcing is the more efficient process, whereas at high latitudes thermal forcing dominates. In between, both forcing processes are roughly equally important. From this we can expect the correction of mechanical forcing in the forecast experiments to have an effect mainly in the tropics. Thermal forcing, on the other hand, should have its largest impact at high latitudes. In middle latitudes, one would expect a combination of both to have the largest response. In practice the results can be expected to be more complicated since smaller scale horizontal as well as vertical modes are involved. Moreover, part of the error might be in the zonal mean gravity mode regime, which, for instance, describes the mean meridional circulation (Hadley cell). Generally, for the zonal mean flow, the separation between Rossby and gravity mode regime is less straightforward than in the non-zonal case, where high frequency gravity modes can usually be identified with noise.

The results of the forecast experiments with modified zonal mean forcing terms are summarised in Fig. 10. It shows vertical cross-sections between 35°S and the north pole of the zonal mean error of temperature (left) and of the zonal wind component (right), averaged over the last 5 days of a 10 day forecast. The two top panels (Fig 10a, 10b) show the errors of the

operational forecast. These fields were used as the basis for the corrective forcing. They agree very well with the wintertime average forecast errors shown in Fig. 1.

The second row of panels gives the error for a forecast where only an additional forcing of the zonal wind field has been applied. The effect on the zonal wind field is shown on the right (Fig. 10d). A large impact can be found in the tropical upper troposphere and stratosphere. In the stratosphere the error has almost disappeared. However, the erroneous strengthening of the mid-latitude jets has only been modestly reduced. The effect of wind forcing on the temperature field is also small (Fig 10c).

We now turn to a forcing of the mass field. Fig. 10e shows the impact on the temperature field. The erroneous cooling at the uppermost model level has been dramatically reduced at all latitudes. This result is not in line with the theoretical predictions as thermal forcing should only be effective at higher latitudes. It can, however, be explained by a significant gravity mode contribution to the zonal mean temperature error at the first model level. Near the north pole, the additional thermal forcing has had an impact on the temperature field at all levels. As apparent from Fig. 10f, the impact of corrective mass field forcing on the momentum can primarily be found between 50°N and 70°N. The tropical wind error is hardly influenced.

Finally, the two bottom panels show that largest improvements are achieved by a combination of thermal and mechanical forcing. The stratospheric wind error (Fig. 10h) has almost completely disappeared. In particular, the large error at the jet-level near 30°S, which could not be removed by either mechanical or thermal corrections, has now gone. Similarly, the temperature errors have been considerably reduced.

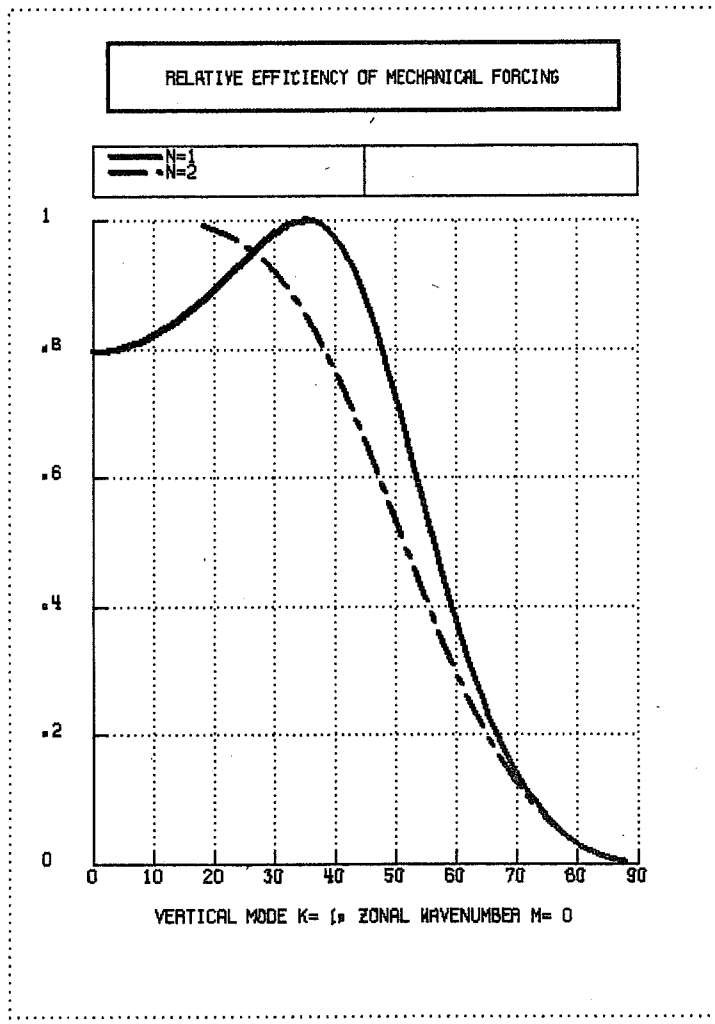

Fig. 9 Efficiency of mechanical forcing η_M for external, zonal wavenumber m=0, gravest symmetric (full) and antisymmetric (dashed-dotted) geostrophic modes.

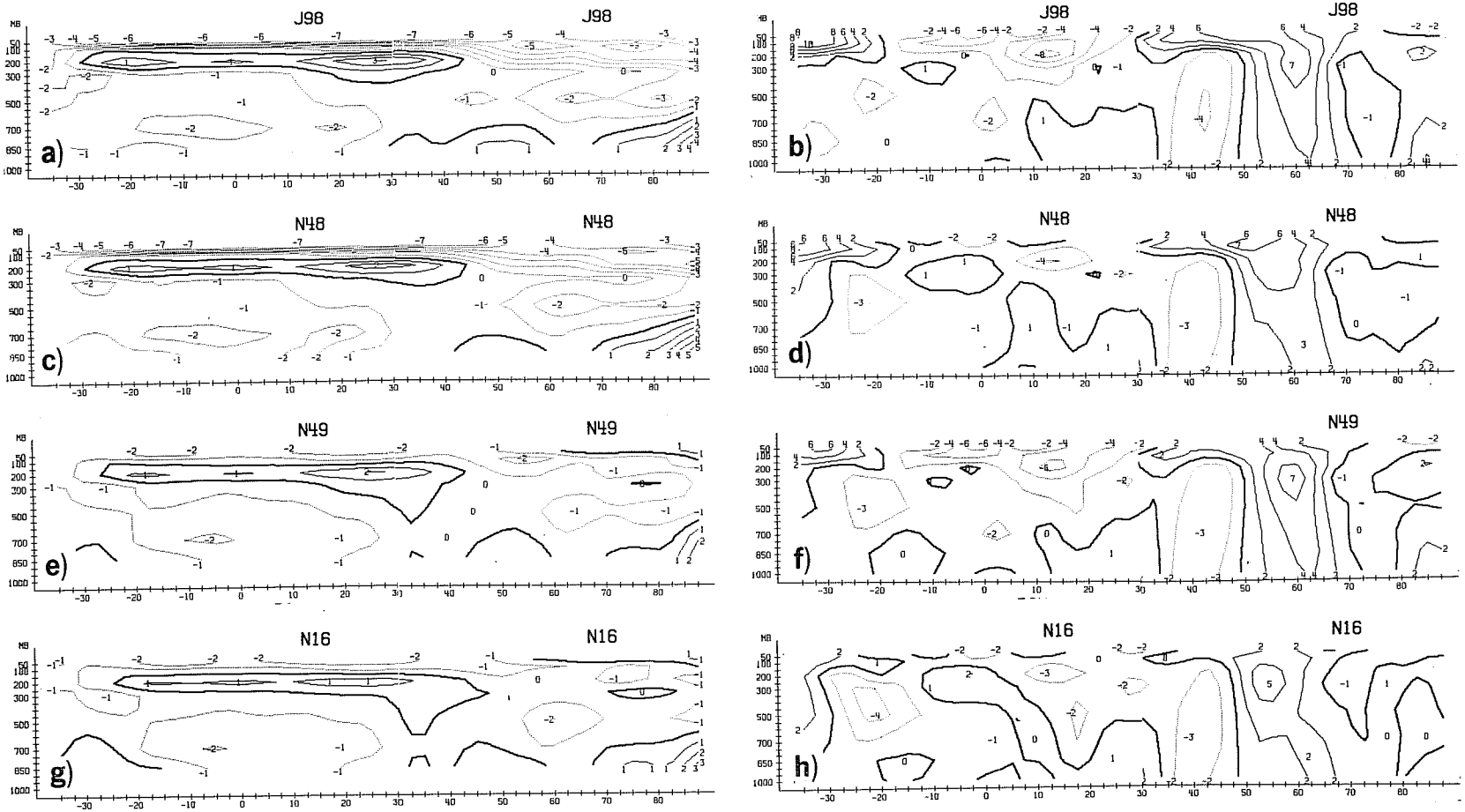

Fig. 10 Zonal mean forecast error between 30°S and 90°N of temperature (left) and zonal wind (right) averaged from day 5 to 10 of the forecast. Panels are for different forecast experiments: a,b) for operational forecast; c,d) for correction in zonal wind forcing; d,e) for correction in massfield forcing; f,g) for correction in mass- and windfield forcing.

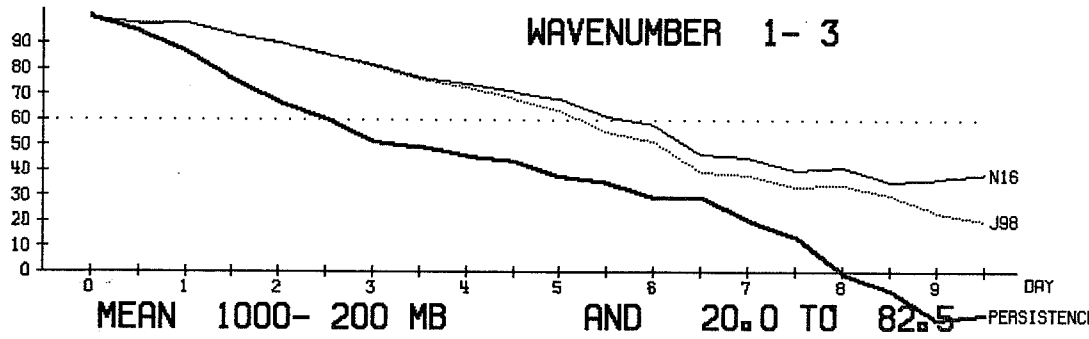

Fig. 11 Anomaly correlation of height, averaged from 1000 hpa to 200 hpa, from 20°N to 82.5 °N and over zonal wavenumber 1 to 3 as a function of time. Dotted line for operational forecast, light line for experimental forecast with corrective mass- and windfield forcing. Heavy line is for persistence forecast.

Another interesting aspect of Fig. 10 is that the improvements are largest in the stratosphere, whereas the improvements in the troposphere are generally smaller. This indicates that the tropospheric 10 day forecast errors were not entirely representative of the linear error growth process. A 5 day error pattern would probably have been less contaminated by nonlinear effects.

By and large, the forecast experiments confirm the theoretical results. Mechanical forcing is efficient in the tropics, thermal forcing at higher latitudes. In middle latitudes, both processes are required in order to be efficient. They also show that a linear correction can lead to a considerable reduction of forecast errors, even in the later part of the forecast. An inclusion of some large-scale, non-zonal waves in the correction process probably would lead to further improvements.

To examine the impact of a better zonal-mean forecast on the prediction of some large scale waves. Fig. 11 shows the anomaly correlation of the height field for zonal wavenumber 1-3 as a function of forecast time, averaged from 1000 hpa to 200 hpa and from 20°N to 82.5°N. The heavy line is for a persistence forecast, the light dotted line for the operational forecast. The light full line shows that the more correct zonal mean forecast has also resulted in an improvement of the prediction of the large scale flow from day 4 onwards.

5. CONCLUSIONS

It has been shown that data assimilation theory can be used in the computation of efficiency parameters for thermal and mechanical forcing in primitive equation models. In a similar way to which observations can be 'rejected' by a model because of a large projection onto gravity wave modes, forcing information can be "lost" if it excites mostly gravity waves.

Examples of this process were given. It was discussed how an erroneous forcing of the balanced flow can lead to a linear error growth during the early part of the forecast. Efficiency parameters for mechanical and thermal forcing were defined, assuming that a forcing is efficient if it has a large weight in forcing Rossby modes. It was discussed how these parameters depend on the horizontal scale and the vertical structure of the forcing as well as on the time scale and on the latitude of the forcing. The impact of the static stability of the atmosphere was investigated.

The efficiency of mechanical forcing increases with increasing vertical, but decreasing horizontal scale. The contrary statements apply to thermal forcing. Thermal forcing efficiency also increases with latitude, whilst decreasing static stability favours thermal forcing. The response of the Rossby regime is largest for quasi-stationary forcing. For small horizontal and large vertical scales, rotational mechanical forcing is the most important process, especially in the tropics. This has implications for the parameterisation of the rotational kinetic energy dissipation and for the representation of orography on these scales. For large scale horizontal, but shallow vertical structures, thermal forcing - such as turbulent transports of latent and sensible heat in the boundary layer - is the dominating process. On intermediate scales, mechanical and thermal forcing are roughly equally important. The implications for the parameterisation of deep convection as both a heat and vorticity source, and for the representation of orography as an obstacle to the flow as well as elevated heat source were discussed. Finally, the theory was verified in forecast experiments.

While the concept of calculating the Rossby mode projection of a particular parameterisation scheme is generally applicable, quantitative statements depend on the various simplifications made in the computation of the model

normal modes. It is, however, thought that the qualitative results are of some relevance.

REFERENCES

Arpe K., A. Hollingsworth, A. Lorenc, M.S. Tracton,S. Uppala, P. Kallberg, 1984: The response of numerical weather prediction systems to FGGE level II-b data. Part II: Forecast verifications and implications for predictability. Submitted to Quart.J.R.Met.Soc.

Bengtsson, L., H. Böttger and M. Kanamitsu, 1982 Simulation of hurricane-type vortices in a general circulation model. Tellus,. 34, 440-457.

Blumen, W., 1972: Geostrophic adjustment. Rev.Geophys.Space Phys., 10, 485-528.

Daley, R., 1980: On the optimal specification of the initial state for deterministic forecasting. Mon.Wea.Rev., 108, 1719-1735.

Daley, R., 1981: Normal mode initialization. Rev.Geophys.Space Phys., 19, 450-468.

Flohn, H., 1953: Hochgebirge und allgemeine Zirkulation. II.Gebirge als Warmequellen. Arch.Met.Geoph.Biokl., 5, 265-279

Frederiksen, J.S., 1982: A unified three-dimensional instability theory of the onset of blocking and cyclogenesis. J.Atmos.Sci., 39, 969-982.

Gill, A.E., 1980: Some simple solutions for heat-induced tropical circulation. Quart.J.R.Met.Soc., 106, 447-462.

Hayashi Y., and D.G. Golder, 1978: The generation of equatorial transient planetary waves: Control experiments with a GFDL general circulation model. J.Atmos.Sci., 35, 2068-2082.

Heckley, W.A., and A.E. Gill, 1984: Some simple analytical solutions to the problem of forced equatorial long waves. Quart.J.R.Met.Soc., 110, 203-217.

Held, I.M. 1983: Stationary and quasi-stationary eddies in the extratropical troposphere: theory. In: Large scale dynamical processes in the atmosphere. Edited by B.J. Hoskins and R.P. Pearce. Academic Press, 127-168.

Huang, R.H., and K. Gambo, 1982 The response of a hemispheric multi-level model atmosphere to forcing by topography and stationary heat sources. II: Forcing by stationary heat sources and forcing by topography and stationary heat sources. J.Met.Soc.Japan, 60, 93-108.

Jacqmin D., and R. Lindzen, 1983: The causation and sensitivity of the winter quasi-stationary planetary waves. Proceedings of IAMAP-WMO symposium on "Maintenance of the quasi-stationary components of the flow in the atmosphere and in atmospheric models", Paris, 79-84.

Kasahara, A., 1976: Normal modes of ultralong waves in the atmosphere. Mon.Wea.Rev., 104, 669-690.

Kasahara, A., 1978: Further studies on a spectral model of the global barotropic primitive equations with Hough harmonic expansions. J.Atmos. Sci., 35, 2043-2051.

Kasahara, A., 1980: Effect of zonal flows on the free oscillations of a barotropic atmosphere. J.Atmos.Sci., 37, 917-929.

Kasahara, A., 1983: The linear response of a stratified global atmosphere to tropical thermal forcing. NCAR MS. 0501/83-13.

Lin B.A., 1982: The behaviour of winter stationary planetary waves forced by topography and diabatic heating. J.Atmos.Sci., 39, 1206-1226.

Lim H., C.P. Chang, 1983: Dynamics of teleconnections and Walker circulations forced by equatorial heating. J.Atmos.Sci., 40, 1897-1915.

Longuet-Higgins, M.S., 1968: The eigenfunctions of Laplace's tidal equations over a sphere. Phil.Trans.Roy.Soc.London. No 1132, A262, 511-607.

Matsuno, T., 1966: Quasi-geostrophic motions in the equatorial area. J. Met.Soc.Japan, 44, 25-42.

McBride, J.L., 1984 Comments on "Simulation of hurricane-type vortices in a general circulation model". Tellus, 36A, 92-93.

Ruprecht,E., and W.M. Gray, 1976: Analysis of satellite-observed tropical cloud clusters. I: Wind and dynamic fields. Tellus, 28, 391-413.

Schubert, W.A., J.J. Hack, P.L. Silva-Dias and S.K. Fulton, 1980 Geostrophic adjustment in an axisymmetric vortex. J.Atmos.Sci., 37, 1464-1484.

Silva-Dias P.L., W.H. Schubert, M. DeMaria, 1983: Large scale response of the tropical atmosphere to transient convection. J.Atmos.Sci., 40, 2689-2707.

Temperton C., and D.L. Williamson, 1981: Normal mode initialization for a multi level grid-point model. Part 1: Linear aspects. Mon.Wea.Rev., 109, 729-743.

Thompson, Jr., R.M., S.W. Payne, E.E. Recker, R.J. Reed, 1979: Structure and properties of synoptic scale wave disturbances in the intertropical convergence zone of the eastern Atlantic. J.Atmos.Sci., 36, 53-72.

Tiedtke, M., 1983: The sensitivity of the time-mean large scale flow to cumulus convection in the ECMWF model. Workshop on "Convection in large-scale numerical models", Reading, ECMWF pp.

Wallace J.M.S., S. Tibaldi, A.J. Simmons, 1983: Reduction of systematic forecast errors in the ECMWF model through the introduction of an envelope orography. Quart.J.R.Met.Soc., 109, 683-717.

Wergen, W., 1981: Nonlinear normal mode initialization of a multi-level fine-mesh model with steep orography. Contr.Phys.Atmos., 54, 389-402.

Wergen,W., 1983: Forced motion in the tropics. Workshop on "Current problems in data assimilation", Reading, ECMWF, 275-298.